J. Phys. Chem. A **2007,** *111,* 8241−8249

Strong Electron Correlation Effects on First- and Second-Order Hyperpolarizabilities in Zwitterionic σ-Conjugated Systems: Its Dependence on Substituents, Conformations, Spacer Size, and Basis Sets

Yuuichi Orimoto[†] **and Yuriko Aoki***[,†,‡]

Department of Material Sciences, Faculty of Engineering Sciences, Kyushu University, 6-1 Kasuga-Park, Fukuoka 816-8580, Japan, and Japan Science and Technology Agency, CREST, 4-1-8 Hon-chou, Kawaguchi, Saitama 332-0012, Japan

Received: April 1, 2007; In Final Form: June 14, 2007

Nonlinear optical properties of zwitterionic σ-conjugated systems were theoretically investigated with relation to the electron correlation effects at the ab initio molecular orbital level. We examined the strong electron correlation effects on the first- and second-order hyperpolarizabilities in the specific systems with effective "π−σ−π" and (or) "π−σ−n" interactions. The electron correlation effects on the hyperpolarizabilities strongly depend on the type of substituents, conformations, spacer size, and basis sets. It was found that the Hartree−Fock level calculations qualitatively predict the behavior of the hyperpolarizabilities after considering the correlation effects. Through-space/-bond interaction analysis quantitatively revealed that the electron correlation effects on the hyperpolarizabilities were induced mainly by the σ-conjugations on the spacer unit in the zwitterionic σ-systems.

Introduction

Nonlinear optical (NLO) materials have been actively studied for their potential applications in the development of new electron-photonic devices.[1−46] In particular, organic π-conjugated systems have been widely investigated as a representative of effective NLO materials due to the strong charge transfer in the system.[19−35] On the other hand, it was reported that even weak conjugated systems also show prominent NLO properties.[36−46] For example, twisted π-systems are suggested as a new NLO material.[37−42] The twisted conformation breaks the π-conjugation between the acceptor and donor units, leading to a charge-separated zwitterionic system. Large hyperpolarizabilities are expected from a large difference in dipole moments between ground and excited states. Interesting NLO behaviors were also reported in the theoretical calculations for zwitterionic σ-conjugated systems.[43−46] The large electron correlation effects on a first-order hyperpolarizability (β) were observed in the specific zwitterionic σ-systems.[45] This is totally different from the NLO behavior of general acceptor−π−donor systems in which the electron correlation effects slightly correct the hyperpolarizabilities at the Hartree−Fock (HF) level. Our previous work using through-space/-bond interaction (TS/TB) analysis[46−53] quantitatively revealed that such abnormally large electron correlation effects on the β value in zwitterionic σ-systems result from intramolecular σ-conjugations.[46] Moreover, it was found that the correlation effects on the β value were controlled by the second-order perturbation energy term between the highest occupied molecular orbital (HOMO) and lowest unoccupied molecular orbital (LUMO) in the perturbation theory treatment for including the electron correlation effects. The electric field dependency of the HOMO−LUMO perturbation energy term mainly causes the strong correlation effects on the β value.

One of the efficient ways to find a new NLO candidate is to design NLO materials at the molecular level. Although it was reported that zwitterionic σ-systems show surprising NLO behaviors, the relationship between the molecular structures and hyperpolarizabilities concerning the electron correlation effects has not been clearly understood. In the present article, we examined the first- and second-order hyperpolarizabilities for various zwitterionic σ-systems. Ab initio MO calculations were performed on the combinations of acceptor−donor groups, conformations, spacer size, and basis sets to investigate the dependency of the NLO response on these factors. To understand the role of σ-conjugations in the NLO behaviors, the TS/TB interaction analysis was applied to the electron correlation effects on the NLO response of the zwitterionic σ-system.

Methods

Calculations of Hyperpolarizabilities. The static first- and second-order hyperpolarizabilities, β_0 and γ_0, are examined by the finite field (FF) method.[54] In a quasi-one-dimensional system, diagonal tensor components β_{XXX} and γ_{XXXX} are considered as the main components of the β_0 and γ_0, where the molecular-axis is assumed on the X-axis. In the FF method, the β_{XXX} and γ_{XXXX} values are numerically calculated as

$$\beta_{XXX} = \frac{\{E(F_X) - E(-F_X)\} - 0.5\{E(2F_X) - E(-2F_X)\}}{{F_X}^3} \quad (1)$$

$$\gamma_{XXXX} = \frac{-6E(0) + 4\{E(F_X) + E(-F_X)\} - \{E(2F_X) + E(-2F_X)\}}{{F_X}^4} \quad (2)$$

respectively. The $E(F_X)$ in eqs 1 and 2 represents the total energy of the system under an applied electric field, F_X. To obtain the

---

* To whom correspondence should be addressed. E-mail: aoki@cube.kyushu-u.ac.jp.

[†] Kyushu University.

[‡] JST, CREST.

10.1021/jp0725376 CCC: $37.00

$E(F_X)$, Hartree−Fock self-consistent field (HF−SCF) calculations were conducted using a Hamiltonian including an electric term, $-r\vec{E}$, where the r and $\vec{E}$ are the operators for electron coordinates and applied electric field, respectively. The FF calculations were performed by the ab initio MO program package GAMESS.[55] The FF method requires considerably accurate total energies because of the numerically differential treatments of eqs 1 and 2. Thus, we adopted the following GAMESS options to keep highly accurate total energies. (a) "ICUT = 20" was used to disregard atomic orbital (AO) integrals less than 10^{-20}. (b) "ITOL = 30" was used to skip the products of primitives whose exponential factor is less than 10^{-30}. (c) "CONV = −10" was used to define 10^{-10} as the SCF density convergence criteria. (d) "FDIFF = .FALSE." option declared that a technique to calculate only the change in the Fock matrices since the previous iteration is not used. The intensity of the applied electric field, $F_X = 0.0007$ au, was adopted.

To confirm the validity of our FF results within the framework of the HF level, we also performed the time-dependent HF (TDHF) method[56] implemented in the GAMESS for the analytic approach to the hyperpolarizabilities. Static hyperpolarizability β_{XXX} with $\omega = 0$ was estimated by using the $TDHF keywords "NFREQ = 1" and "FREQ(1) = 0.0" to specify the use of only one frequency, $\omega = 0.0$ au.

In this work, the electron correlation effects are considered by the Møller−Plesset second-order perturbation theory (MP2) methods[57] after the HF−SCF procedures. The frozen core approximation was adopted for the MP2 calculations for efficiency. In this approximation, chemical core orbitals are omitted from the calculations. We confirmed in Results and Discussion that this approximation does not affect the results.

Through-Space/-Bond Interaction Analysis. The TS/TB interaction analysis[46−53] was developed to analyze the specific intramolecular interactions quantitatively at the ab initio MO level. The procedures for the TS/TB analysis are as follows:

(i) AO integrals are calculated for two types of basis functions. One is for conventional basis functions; the other one is for artificially contracted basis functions with extremely large exponents in the Gaussian-type functions, $\exp(-\alpha r^2)$.

(ii) To delete the specific orbital interactions, a new integrals file for the TS/TB analysis is obtained by merging the two AO integrals files in procedure i. The integral elements corresponding to the remaining interactions are extracted from the conventional AO integrals file. On the other hand, the integral elements corresponding to deleting interactions are extracted from the artificial AO integrals file.

(iii) The HF−SCF calculation using the new integrals file provides us a total energy after deleting the specific interactions.

(iv) The TS/TB analysis was linked with Møller−Plesset perturbation methods to include the electron correlation effects.

By comparing a "deletion" state after eliminating the specific interactions with a conventional "full interaction" state, we can quantitatively estimate the contributions of the interactions to the total energy, electronic structures, and so on. The TS/TB treatment was also linked with the FF method to analyze the relationship between orbital interactions and hyperpolarizabilities.[46] Because the total energy under an applied electric field was calculated after deleting the specific interactions, we can examine the contribution of the interactions to the hyperpolarizabilities. That is, hyperpolarizabilities after deleting the interactions, $\beta_{XXX}{}^{\text{delete}}$ and $\gamma_{XXXX}{}^{\text{delete}}$, can be estimated by eqs 1 and 2 using $E(0)^{\text{delete}}$, $E(F_X)^{\text{delete}}$, $E(-F_X)^{\text{delete}}$, $E(2F_X)^{\text{delete}}$, and $E(-2F_X)^{\text{delete}}$ calculated under considering the deletions. The contributions of the interactions to the hyperpolarizabilities are examined by comparing these values, $\beta_{XXX}{}^{\text{delete}}$ and $\gamma_{XXXX}{}^{\text{delete}}$, with conventional ones, $\beta_{XXX}{}^{\text{conv}}$ and $\gamma_{XXXX}{}^{\text{conv}}$. All the procedures described above were incorporated into the program package GAMESS.

The difference of the TS/TB analysis and other methods for analyzing orbital interactions was discussed in ref 51. Advantages of the TS/TB analysis are as follows: (a) Electron correlation effects are easily introduced in the analyses due to AO integral-based treatments. (b) Two-electron integrals corresponding to the interactions we want to eliminate are completely deleted. (c) Wave functions in the "deletion" states satisfy the SCF.

Model Molecules

Figure 1a shows the structures of acceptor, spacer, and donor units for zwitterionic σ-conjugated systems. The notation of the "acceptor" (**1**−**5**) and "donor" (**a**−**c**) are defined for the system under an applied electric field. All the acceptor units have a positive charge, whereas all the donor units have a negative charge. In this work, polyethylene (PE) with all-trans structure is selected as a σ-conjugated spacer unit. The spacer part is abbreviated as PE$_n$, where the index "n" is the number of $-CH_2-CH_2-$ units. The acceptor $-N^+H_2CH_3$ (**5**) is considered as a reference unit for $-N^+H{=}CH_2$ (**1**) to examine the effects of π-orbitals. We considered all the combinations between the acceptor (**1**−**4**) and donor (**a**−**c**) units as listed in Table 1.

Figure 1b shows the Fisher's diagrams describing the conformations of the zwitterionic σ-systems. The left and right diagrams in panel b correspond to the views from the acceptor $-N^+H{=}CH_2$ (**1**) and donor $-CO_2^-$ (**b**) sides, respectively. The torsion angles ϕ_1 and ϕ_2 are defined by the dihedral angles $\angle ijkl$ and $\angle rstu$, respectively. The letters $\{i, j\}$ and $\{r, s\}$ are shown in the acceptor and donor units in panel a, respectively. The k, l, t, and u are depicted in the "spacer" unit in the same panel. It should be noted that the ϕ_2 cannot be defined for donor $-O^-$ (**c**). The bend angle ϕ_{bend} in the right diagram of panel b indicates a deviation from the sp^2 plane of the donor units. Thus, large ϕ_{bend} means the change in hybridization from sp^2 to sp^3 in the donor unit.

All the geometrical parameters of the molecules in Table 1 were fully optimized at the level of restricted HF (RHF)/6-31G(d). Optimized calculations at the HF level are not enough to determine the geometries of the zwitterionic system, and the incorrect geometries slightly affect the hyperpolarizability. However, to save cost, the electron correlation effects were not considered for the optimizations as a first step of the analysis. Ab initio MO calculations for the geometry optimizations were performed by the Gaussian03 program package.[58]

Results and Discussion

Geometries and Electronic Structures of Zwitterionic σ-Conjugated Systems. Table 1 lists the geometrical parameters of various zwitterionic σ-systems optimized at the RHF/6-31G(d) level. We first consider the conformations of the acceptor units. In the acceptors $-N^+H{=}CH_2$ (**1**) and $-N^+C_5H_5$ (**4**) units, the acceptors' plane has a tendency to be nearly perpendicular to the molecular plane of the spacer unit; e.g., $\phi_1 \approx 90°$. Thus, it was expected that the π-orbitals of the acceptor unit effectively overlap with the σ-orbitals of the C−C bonds in the PE spacer (refer to Figure 1b). In contrast, model **5c** with the $-N^+H_2CH_3$ unit shows a different tendency from the models with $-N^+H{=}CH_2$ and $-N^+C_5H_5$ that the acceptors' plane and the spacer plane are located in the "periplanar" position; that is, $\phi_1 \approx 180°$.

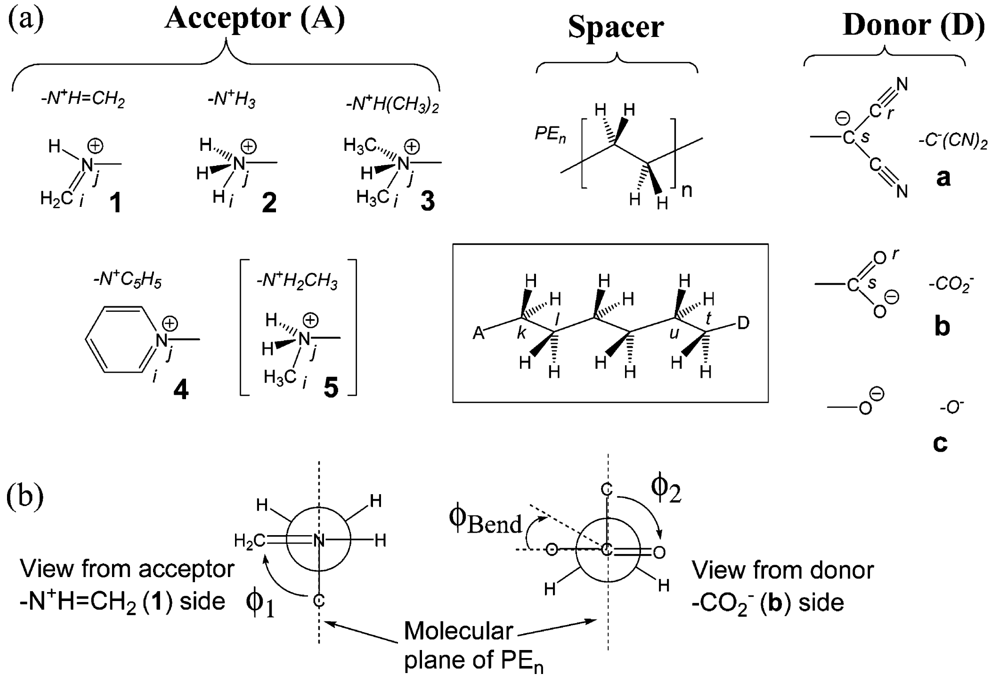

Figure 1. (a) Structures of acceptor (**1**−**5**), spacer, and donor (**a**−**c**) units for zwitterionic σ-conjugated systems. Italics next to the structures represent the abbreviations for the units. The $-N^+H_2CH_3$ (**5**) in parentheses is a reference model for $-N^+H{=}CH_2$ (**1**). The figure in the box shows the assignments of atoms for the definition of the dihedral angles, ϕ_1 and ϕ_2. (b) Fisher diagrams describing the ϕ_1, ϕ_2, and bend angle ϕ_{bend}. The ϕ_{bend} corresponds to the deviation from the sp^2 plane of the donor unit.

TABLE 1: Conformations of Zwitterionic σ-Systems Obtained by Geometry Optimizations at the HF/6-31G(d) Basis Set

molecule	spacer	acceptor	donor	$\phi_1{}^a$ (deg)	$\phi_2{}^a$ (deg)	$\phi_{\text{bend}}{}^b$ (deg)
1a	PE_3	$-N^+H{=}CH_2$ (**1**)	$-C^-(CN)_2$ (**a**)	116.5	77.5	8.6
1b	PE_3	$-N^+H{=}CH_2$ (**1**)	$-CO_2^-$ (**b**)	116.8	−3.3	0.2
1c (=**1c**$_3$)	PE_3	$-N^+H{=}CH_2$ (**1**)	$-O^-$ (**c**)	115.4		
2a	PE_3	$-N^+H_3$ (**2**)	$-C^-(CN)_2$ (**a**)	58.8	86.5	11.7
2b	PE_3	$-N^+H_3$ (**2**)	$-CO_2^-$ (**b**)	59.4	−3.8	0.3
2c	PE_3	$-N^+H_3$ (**2**)	$-O^-$ (**c**)	59.2		
3a	PE_3	$-N^+H(CH_3)_2$ (**3**)	$-C^-(CN)_2$ (**a**)	168.6	85.7	11.5
3b	PE_3	$-N^+H(CH_3)_2$ (**3**)	$-CO_2^-$ (**b**)	168.1	−3.6	0.2
3c	PE_3	$-N^+H(CH_3)_2$ (**3**)	$-O^-$ (**c**)	167.1		
4a	PE_3	$-N^+C_5H_5$ (**4**)	$-C^-(CN)_2$ (**a**)	88.4	85.4	11.2
4b	PE_3	$-N^+C_5H_5$ (**4**)	$-CO_2^-$ (**b**)	88.0	0.1	0.0
4c	PE_3	$-N^+C_5H_5$ (**4**)	$-O^-$ (**c**)	87.4		
5c	PE_3	$-N^+H_2CH_3$ (**5**)	$-O^-$ (**c**)	179.8		
1c$_4$	PE_4	$-N^+H{=}CH_2$ (**1**)	$-O^-$ (**c**)	117.1		
1c$_5$	PE_5	$-N^+H{=}CH_2$ (**1**)	$-O^-$ (**c**)	117.3		

[a] Torsional angles ϕ_1 and ϕ_2 are shown in Figure 1b. The ϕ_2 is not defined for $-O^-$ (**c**). [b] Bend angles ϕ_{bend} are defined only for donor units and described in the right-hand figure of Figure 1b. ϕ_{bend} is not defined for $-O^-$ (**c**).

Such a conformational difference implies that the stabilizations due to $\pi-\sigma$ interactions are strong in the $-N^+H{=}CH_2$ and $-N^+C_5H_5$ systems. It was found that the spacer size dependency on the ϕ_1 is negligibly small by comparing the ϕ_1 of **1c** (=**1c**$_3$), **1c**$_4$, and **1c**$_5$. This means that the direct through-space interactions between the acceptor and donor units are very weak.

Next, the conformations of the donor units are considered. $\phi_{\text{bend}} \approx 10°$ was found in the $-C^-(CN)_2$ unit (**a**). It means that sp^3 properties mixed into the sp^2 hybridizations in the donor unit. That is, the carbon atom with a negative charge in $-C^-(CN)_2$ includes a lone pair orbital (n-orbital) property. The dihedral angle $\phi_2 \approx 90°$ in the $-C^-(CN)_2$ unit results in $\pi-\sigma$ and (or) n$-\sigma$ interactions between the donor unit and the spacer C−C single bonds. It should be noted that we use an expression “and (or)” throughout this work because of the mixed state of π- and n-orbitals. Similarly to the $-C^-(CN)_2$ unit, models with the $-O^-$ unit (**c**) are expected to have $\pi-\sigma$ and (or) n$-\sigma$ interactions. On the other hand, the $\phi_2 \approx 0°$ in the $-CO_2^-$ unit (**b**) implies that there are small $\pi-\sigma$ interactions between the donor $-CO_2^-$ and the spacer C−C bonds due to the orthogonality between π- and σ-orbitals.

By considering the conformations of both acceptor and donor units, we can conclude that the effective $\pi-\sigma-\pi$ and (or) $\pi-\sigma-$n interactions are expected in models **1a**, **1c** (=**1c**$_3$), **4a**, **4c**, **1c**$_4$, and **1c**$_5$.

To confirm the zwitterionic electronic structures of the models in Table 1, the Mulliken’s net charges and dipole moment (μ_X) were calculated for these models at the HF/6-31+G(d) level on the basis of the HF/6-31G(d) optimized geometries. The results were listed in Table 2, where the net charges on the atoms were summed up for each acceptor, spacer, or donor unit. It was found that all the models have zwitterionic properties; that is, the acceptor unit was positively charged, while the donor unit was negatively charged. The spacer unit is positively charged except for **4b** and **4c** in which the spacer unit keeps a

TABLE 2: Mulliken Net Charges[a] and Dipole Moment μ_X (in au) for Zwitterionic σ-Systems at the HF/6-31+G(d) Level[b]

molecules[c]	acceptor	spacer	donor	μ_X (au)
1a	+0.682	+0.411	−1.093	−17.09
1b	+0.677	+0.160	−0.837	−16.46
1c (=**1c**$_3$)	+0.672	+0.177	−0.849	−14.59
2a	+0.500	+0.584	−1.084	−16.42
2b	+0.497	+0.336	−0.833	−15.84
2c	+0.492	+0.357	−0.849	−13.99
3a	+0.642	+0.444	−1.086	−16.91
3b	+0.634	+0.201	−0.835	−16.31
3c	+0.631	+0.216	−0.847	−14.45
4a	+0.891	+0.215	−1.106	−17.78
4b	+0.892	−0.057	−0.835	−17.16
4c	+0.848	+0.001	−0.849	−15.27
5c	+0.543	+0.304	−0.847	−14.37
1c$_4$	+0.682	+0.171	−0.853	−19.30
1c$_5$	+0.686	+0.168	−0.854	−24.07

[a] Net charges were summed up for each acceptor, spacer, or donor unit. [b] HF/6-31G(d) optimized geometries were used. [c] Refer to Table 1.

nearly neutral charge. The large dipole moments, μ_X, in Table 2 were produced by the charge separation in these models.

Electron Correlation and Basis Set Effects on Hyperpolarizabilities in Zwitterionic σ-Systems. Table 3 shows the main components of the static first-order hyperpolarizability, β_{XXX}, for various zwitterionic σ-systems listed in Table 1. The β_{XXX} values were calculated by the FF method at the 3-21G, 6-31G(d), and 6-31+G(d) levels on the basis of the HF/6-31G(d) optimized geometries. To investigate the electron correlation effects on the β_{XXX} values, we compared the β_{XXX} values by the HF and MP2 methods. The notation "MP2/HF" in Table 3 indicates the ratio of the MP2 results to the HF results.

First, the results for the 6-31+G(d) basis set were considered. The order of the β_{XXX} values was **1a** > **1c** > **4c** > **4a** ≫ others in the HF/6-31+G(d) results. The **1a**, **1c**, **4a**, and **4c** showing large β_{XXX} values correspond to the models in which we expect the $\pi-\sigma-\pi$ and (or) $\pi-\sigma-$n interactions as mentioned in the above subsection. Thus, it was concluded that the $\pi-\sigma-\pi$ and (or) $\pi-\sigma-$n interactions play an important role on the first-order hyperpolarizability. In the MP2/6-31+G(d) results, the β_{XXX} values were increased in all the models compared with the HF results due to the consideration of the electron correlation effects (see "MP2/HF" terms). In particular, a remarkable increase of the β_{XXX} value was observed in **1a**, **1c**, **4a**, and **4c**; the MP2/HF value was ×7.6 to ×8.8 for these models. The β_{XXX} values in the MP2 results show the same order as those in the HF results; that is, **1a** > **1c** > **4c** > **4a** ≫ others. This implies that the order of the β_{XXX} values in the MP2 results with high computational costs can be qualitatively estimated by the order of the β_{XXX} values in the HF results with small costs.

Next, to examine the basis set effects, the 6-31+G(d) results were compared with those for the 6-31G(d) and 3-21G basis sets. The order of β_{XXX} values was **1c** > **4c** > **1a** > **4a** ≫ others in the HF/6-31G(d) results. The MP2/6-31G(d) results show the same order of β_{XXX} values as the HF/6-31G(d) results. The order of β_{XXX} values in the 3-21G results was the same as that in the 6-31G(d) results; that is, **1c** > **4c** > **1a** > **4a** ≫ others, although the absolute magnitudes of the β_{XXX} values in the 3-21G results were much larger than those in the other basis sets. Within the framework of the 6-31G(d) or 3-21G basis set, the HF results qualitatively estimated the order of β_{XXX} in the MP2 results. However, the β_{XXX} values for **1c** and **4c** were overestimated in both the 6-31G(d) and 3-21G results compared with the 6-31+G(d) results. Therefore, it was found that diffuse functions involved in the 6-31+G(d) basis set are required for estimating the β_{XXX} values in **1c** and **4c**. Especially, the expanding anionic orbitals of donor $-\mathrm{O}^-$ unit in the **1c** and **4c** should be described by using the diffused basis functions.

Table 4 shows the main components of the static second-order hyperpolarizability, γ_{XXXX}, for the zwitterionic σ-systems. The γ_{XXXX} values were calculated by the same way as the β_{XXX} values. In both the HF/6-31+G(d) and MP2/6-31+G(d) results, the order of γ_{XXXX} values was **1a** > **1c** > **4a** > **4c** ≫ others. Similarly to the β_{XXX} case, the HF results well estimated the order of γ_{XXXX} values in the MP2 results. The order of γ_{XXXX} values is the nearly same as that of β_{XXX} values at the same basis set; that is, **1a** > **1c** > **4c** > **4a** ≫ others. The only difference in the order between β_{XXX} and γ_{XXXX} values was the inversion of **4a** and **4c**. A remarkable increase of the γ_{XXXX} value was observed in **1a**, **1c**, **4a**, and **4c**; the MP2/HF value was ×10.4 to ×11.7 for these models. In the HF/6-31G(d) and MP2/6-31G(d) results, the order of the γ_{XXXX} values was **1c** > **1a** > **4c** > **4a** ≫ others. On the other hand, the order of γ_{XXXX} values was **1c** > **4c** > **1a** > **4a** ≫ others in the HF/3-21G and MP2/3-21G results. In both the 6-31G(d) and 3-21G results, the γ_{XXXX} values of **1c** and **4c** were overestimated compared to the 6-31+G(d) results due to the lack of diffuse functions.

The absolute magnitudes of the β_{XXX} and γ_{XXXX} values strongly depend on the basis set and were different from each other among 3-21G, 6-31G(d), and 6-31+G(d) basis sets. However, it is worth mentioning that the HF/3-21G results provide us NLO candidates with large hyperpolarizabilities, e.g., **1a**, **1c**, **4a**, and **4c** predicted by MP2/6-31+G(d) results.

To know the effects of the frozen core approximation on the MP2 results, the β_{XXX} and γ_{XXXX} values of **1a**, **1b**, **1c**, and **5c** were calculated at the level of 6-31+G(d)//HF/6-31G(d) without using the approximation (see Table 5a,b). By comparing them with the results in Tables 3 and 4, it was found that the frozen core approximation does not change the values of hyperpolarizabilities. On the other hand, the basis set size convergence of β_{XXX} and γ_{XXXX} values was examined by calculating the hyperpolarizabilities using larger basis sets, 6-31+G(d,p), 6-31++G(d), and 6-31++G(d,p) (see Table 5c,d). It was found that these results were very similar to the 6-31+G(d) results in Tables 3 and 4. Therefore, we can conclude that the results by the 6-31+G(d) basis set with the frozen core approximation are adequate for examining the hyperpolarizabilities of zwitterionic σ-systems.

Spacer Size Dependency of Hyperpolarizabilities in Zwitterionic σ-Systems. The spacer size dependency of the β_{XXX} and γ_{XXXX} values was examined for **1c** (=**1c**$_3$), **1c**$_4$, and **1c**$_5$ by using the FF method at the 3-21G, 6-31G(d), and 6-31+G(d) levels based on the HF/6-31G(d) optimized geometries. The results for β_{XXX} and γ_{XXXX} values are shown in Table 6a,b, respectively.

First, we considered the spacer size dependency of the β_{XXX} values (see Table 6a). As the spacer size increases, the β_{XXX} value decreases in the HF/6-31+G(d), while increasing in MP2/6-31+G(d) results. This means that the HF method cannot describe even qualitatively the spacer size dependency of the β_{XXX} values in the MP2 results. In addition, the MP2/HF value largely increases as the spacer size increases. Thus, the correlation effects should be included for obtaining correct β_{XXX} values of the system with a large spacer. In contrast, in the 6-31G(d) and 3-21G basis sets, the β_{XXX} values of both the HF and MP2 methods increase with the spacer size. Thus, within these basis sets, the HF results provide us qualitatively correct descriptions of β_{XXX} values in the MP2 results. However, the

TABLE 3: Main Components of First-Order Hyperpolarizability, β_{XXX} (in $\times$ 10^3 au), for Zwitterionic σ-Systems Obtained at the 3-21G, 6-31G(d), and 6-31+G(d) Levels[a]

	3-21G			6-31G(d)			6-31+G(d)		
molecules[b]	HF	MP2[c]	MP2/HF[d]	HF	MP2[c]	MP2/HF[d]	HF	MP2[c]	MP2/HF[d]
1a	12.71	138.27	×10.9	4.12	36.12	×8.8	4.35	38.35	×8.8
1b	1.23	5.37	×4.4	0.83	2.81	×3.4	0.70	2.26	×3.2
1c	38.11	576.61	×15.1	5.92	58.87	×9.9	3.84	32.82	×8.5
2a	0.47	1.16	×2.4	0.48	1.20	×2.5	0.84	4.15	×5.0
2b	0.38	0.82	×2.2	0.39	0.82	×2.1	0.34	0.82	×2.4
2c	0.68	2.20	×3.2	0.61	1.90	×3.1	1.11	5.80	×5.2
3a	0.47	1.03	×2.2	0.45	0.95	×2.1	0.41	1.04	×2.5
3b	0.41	0.82	×2.0	0.40	0.78	×2.0	0.32	0.64	×2.0
3c	0.61	1.63	×2.7	0.52	1.29	×2.5	0.54	1.50	×2.8
4a	8.47	86.07	×10.2	2.96	24.12	×8.2	2.48	18.87	×7.6
4b	1.05	4.71	×4.5	0.71	2.51	×3.5	0.63	2.02	×3.2
4c	29.48	430.20	×14.6	4.46	42.40	×9.5	2.53	19.20	×7.6
5c	0.61	1.67	×2.7	0.53	1.35	×2.5	0.58	1.86	×3.2

[a] All the calculations were performed by the FF method based on the HF/6-31G(d) optimized geometries. [b] Refer to Table 1. [c] Frozen core approximation was adopted. [d] “MP2/HF” represents the ratio of the MP2 result to the HF result.

TABLE 4: Main Components of Second-Order Hyperpolarizability, γ_{XXXX} (in $\times 10^5$ au), for Zwitterionic σ-Systems Obtained at the 3-21G, 6-31G(d), and 6-31+G(d) Levels[a]

	3-21G			6-31G(d)			6-31+G(d)		
molecules[b]	HF	MP2[c]	MP2/HF[d]	HF	MP2[c]	MP2/HF[d]	HF	MP2[c]	MP2/HF[d]
1a	136.45	1850.61	×13.6	32.62	382.44	×11.7	38.77	445.43	×11.5
1b	3.50	26.60	×7.6	1.44	9.53	×6.6	1.35	6.88	×5.1
1c	358.25	6759.80	×18.9	37.21	489.67	×13.2	22.23	259.97	×11.7
2a	0.60	1.94	×3.3	0.64	2.13	×3.3	4.61	34.32	×7.5
2b	0.27	1.15	×4.3	0.27	1.10	×4.1	0.51	1.83	×3.6
2c	1.04	5.54	×5.3	0.86	4.53	×5.3	4.40	34.94	×7.9
3a	0.44	1.51	×3.4	0.40	0.96	×2.4	0.72	2.56	×3.5
3b	0.26	0.81	×3.1	0.24	1.03	×4.3	0.38	2.15	×5.7
3c	0.62	2.30	×3.7	0.44	1.67	×3.8	0.77	3.24	×4.2
4a	90.32	1149.57	×12.7	22.99	253.70	×11.0	18.72	193.88	×10.4
4b	3.19	22.80	×7.2	1.36	9.15	×6.7	1.23	5.85	×4.7
4c	309.61	5576.57	×18.0	29.22	369.08	×12.6	13.20	143.00	×10.8
5c	0.66	2.85	×4.3	0.48	1.68	×3.5	1.02	5.34	×5.2

[a] All the calculations were performed by the FF method based on the HF/6-31G(d) optimized geometries. [b] Refer to Table 1. [c] Frozen core approximation was adopted. [d] “MP2/HF” represents the ratio of the MP2 result to the HF result.

β_{XXX} values in the 6-31G(d) and 3-21G results were considerably overestimated and enlarged explosively as the spacer size increases. The difference in the β_{XXX} behavior among these basis sets is mainly related to the consideration of diffuse functions.

Next, the spacer size dependency of the γ_{XXXX} values was considered (see Table 6b). In the 6-31+G(d) results, the γ_{XXXX} values monotonously increase with the increase of the spacer size in both the HF and MP2 results. Similarly to the β_{XXX} values, the MP2/HF value increases accompanying the increase of the spacer size. Thus, the electron correlation effects become a more important factor for estimating the γ_{XXXX} values of the system with larger spacer unit. The spacer size dependency by 6-31G(d) and 3-21G is qualitatively similar to the 6-31+G(d) results. The only exception was that the MP2/HF value does not monotonously increase in the 3-21G results with the spacer size.

There is no direct relationship between the hyperpolarizabilities and the charge distribution under no electric field. However, the polarization of the system can be considered as one of the efficient indices for predicting the NLO properties. Thus, to examine the relationship between the charge distribution and the spacer size dependency of the β_{XXX} and γ_{XXXX} values, the Mulliken's net charges and dipole moment, μ_X, were calculated for **1c** (=**1c**$_3$), **1c**$_4$, and **1c**$_5$, and also listed in Table 2 (HF/6-31+G(d)//HF/6-31G(d)). It was found that the charge separation between the acceptor and donor units was slightly accelerated by the enlargement of the spacer length. Moreover, the neutralization of the spacer unit was also observed with the spacer length. The charge separation increases the absolute values of the dipole moment, μ_X, and the polarization is related to the spacer size dependency of the β_{XXX} and γ_{XXXX} values.

Conformation Dependency of Hyperpolarizabilities in Zwitterionic σ-Systems. We estimated the torsion angles ϕ_1 and ϕ_2 dependency of the hyperpolarizabilities for **1a**−**c** and **5c** to examine conformational effects on the β_{XXX} and γ_{XXXX} values. These calculations were conducted by the FF method at both the HF/6-31+G(d) and MP2/6-31+G(d) levels on the basis of the HF/6-31G(d) optimized geometries (see Figure 2).

First, to examine the effect of π-orbitals in the acceptor unit, ϕ_1 dependency of hyperpolarizabilities for **1c** and **5c** were compared in panels a for β_{XXX} and b for γ_{XXXX}. Only ϕ_1 was changed under the fixed geometry in the other parameters. It was found that the hyperpolarizabilities for **1c** remarkably changed depending on ϕ_1 in the MP2 results. The β_{XXX} and γ_{XXXX} values have a maximum at $\phi_1 = 90°$, and monotonously decrease with a deviation from the angle. At the angles $\phi_1 = 0$ and 180°, the β_{XXX} and γ_{XXXX} values become nearly zero. This means that the hyperpolarizabilities in **1c** were controlled by the “π−σ” orbital overlap between the π-orbitals of the $-N^+H{=}CH_2$ and the σ-orbitals of C−C bonds in the spacer unit. The arrows in the panels indicate the optimized ϕ_1 for **1c**. The hyperpolarizabilities of **1c** at the HF level have ϕ_1 dependency similar to the MP2 results, though their absolute magnitudes

TABLE 5: Calculation Level Convergency of the First-Order, β_{XXX} Hyperpolarizabilities (in $\times$ 10^3 au), and Second-Order Hyperpolarizabilities, γ_{XXX} (in $\times$ 10^5 au), for 1a−c and 5c[a]

	(a) β_{XXX} at the 6-31+G(d) Level [Without Frozen Core Approximation] 6-31+G(d)			(b) γ_{XXXX} at the 6-31+G(d) Level [Without Frozen Core Approximation] 6-31+G(d)		
molecule[b]	HF	MP2[c]	MP2/HF[e]	HF	MP2[c]	MP2/HF[e]
1a	4.35	38.36	×8.8	38.77	445.56	×11.5
1b	0.70	2.26	×3.2	1.35	6.88	×5.1
1c	3.84	32.84	×8.6	22.23	260.17	×11.7
5c	0.58	1.86	×3.2	1.02	5.33	×5.2

(c) β_{XXX} Obtained with Larger Basis Sets

	6-31+G(d,p)			6-31++G(d)			6-31++G(d,p)		
molecule[b]	HF	MP2[d]	MP2/HF[e]	HF	MP2[d]	MP2/HF[e]	HF	MP2[d]	MP2/HF[e]
1a	4.37	39.32	×9.0	4.27	37.51	×8.8	4.29	38.43	×9.0
1b	0.70	2.25	×3.2	0.70	2.23	×3.2	0.69	2.23	×3.2
1c	3.80	32.67	×8.6	3.61	30.53	×8.5	3.57	30.39	×8.5
5c	0.58	1.85	×3.2	0.55	1.75	×3.2	0.55	1.75	×3.2

(d) γ_{XXXX} Obtained with Larger Basis Sets

	6-31+G(d,p)			6-31++G(d)			6-31++G(d,p)		
molecule[b]	HF	MP2[d]	MP2/HF[e]	HF	MP2[d]	MP2/HF[e]	HF	MP2[d]	MP2/HF[e]
1a	39.11	458.39	×11.7	37.76	433.77	×11.5	38.06	446.15	×11.7
1b	1.34	8.30	×6.2	1.33	7.97	×6.0	1.32	8.22	×6.2
1c	21.95	258.20	×11.8	20.51	237.76	×11.6	20.24	236.37	×11.7
5c	1.01	5.02	×5.0	0.94	4.74	×5.0	0.94	4.57	×4.9

[a] All the calculations were performed by the FF method based on the HF/6-31G(d) optimized geometries. [b] Refer to Table 1. [c] All the orbitals were considered in the MP2 calculations. [d] Frozen core approximation was adopted. [e] The ratio of the MP2 result to the HF result.

TABLE 6: Spacer Size Dependency of the First-Order, β_{XXX} (in $\times 10^3$ au), and Second-Order Hyperpolarizabilities, γ_{XXXX} (in $\times 10^5$ au), for 1c (=1c$_3$), 1c$_4$, and 1c$_5$[a]

(a) β_{XXX}

	3-21G			6-31G(d)			6-31+G(d)		
molecule[b]	HF	MP2[c]	MP2/HF[d]	HF	MP2[c]	MP2/HF[d]	HF	MP2[c]	MP2/HF[d]
1c (=**1c**$_3$)	38.11	576.61	×15.1	5.92	58.87	×9.9	3.84	32.82	×8.5
1c$_4$	213.64	7069.65	×33.1	5.85	86.14	×14.7	3.03	33.93	×11.2
1c$_5$	1582.33	47544.49	×30.1	7.63	231.36	×30.3	2.42	39.54	×16.3

(b) γ_{XXXX}

	3-21G			6-31G(d)			6-31+G(d)		
molecule[b]	HF	MP2[c]	MP2/HF[d]	HF	MP2[c]	MP2/HF[d]	HF	MP2[c]	MP2/HF[d]
1c (=**1c**$_3$)	358.25	6759.80	×18.9	37.21	489.67	×13.2	22.23	259.97	×11.7
1c$_4$	4501.19	162957.24	×36.2	68.82	1339.67	×19.5	28.99	469.11	×16.2
1c$_5$	31634.07	583741.93	×18.5	155.32	5761.33	×37.1	34.19	840.57	×24.6

[a] All the calculations were performed by the FF method based on the HF/6-31G(d) optimized geometries. [b] Refer to Table 1. [c] Frozen core approximation was adopted. [d] The ratio of the MP2 result to the HF result.

are considerably small. In contrast, model **5c** exhibits small and nearly constant hyperpolarizabilities regardless of ϕ_1. Thus, the $\sigma-\sigma$ interactions between $-N^+H_2CH_3$ and the spacer unit in **5c** are negligibly small and do not contribute to the hyperpolarizabilities. From the comparison between **1c** and **5c**, it was concluded that the $\pi-\sigma$ interactions in **1c** effectively produce the large hyperpolarizabilities, β_{XXX} and γ_{XXXX}, at the suitable conformation near $\phi_1 = 90°$ when considering the electron correlation effects.

Next, the ϕ_2 dependency in the hyperpolarizabilities of **1a**,**b** are shown in panels c for β_{XXX} and d for γ_{XXXX} to know the contributions of donors $-C^-(CN)_2$ and $-CO_2^-$ to the hyperpolarizabilities. In panels c and d, only ϕ_2 was changed under the fixed geometry in the other parameters. The hyperpolarizabilities of **1a** at the MP2 level show the strong ϕ_2 dependency. The values have a maximum at $\phi_2 = 90°$ and disappear at $\phi_2 = 0$ and 180°. The arrows in these panels depict the optimized ϕ_2 for **1a**. The HF results of **1a** show small hyperpolarizabilities depending on the conformation. By considering the results of the ϕ_1 dependency in **1c** and the ϕ_2 dependency in **1a**, large β_{XXX} and γ_{XXXX} values were produced not only by the $\pi-\sigma$ interactions at the acceptor side but also by the $\sigma-\pi$ and (or) σ−n interactions at the donor side. Conversely to **1a**, model **1b** shows small and constant hyperpolarizabilities regardless of ϕ_2 at both levels of HF and MP2. This means that π-orbitals of $-CO_2^-$ in **1b** cannot make efficient $\pi-\sigma$ interactions to the C−C σ-orbitals of the spacer unit. The geometry of **1b**, in which the donor and spacer units keep nearly a coplanar structure, also supports the weak $\pi-\sigma$ interactions (see Table 1).

To examine the validity of our calculations using the FF method, the TDHF method with $\omega = 0$ was applied to the estimations of β_{XXX} values for **1c** and **5c** at the HF/6-31+G(d) level on the basis of the HF/6-31G(d) geometries. The FF and TDHF results were compared in Figure 2e. It was found that

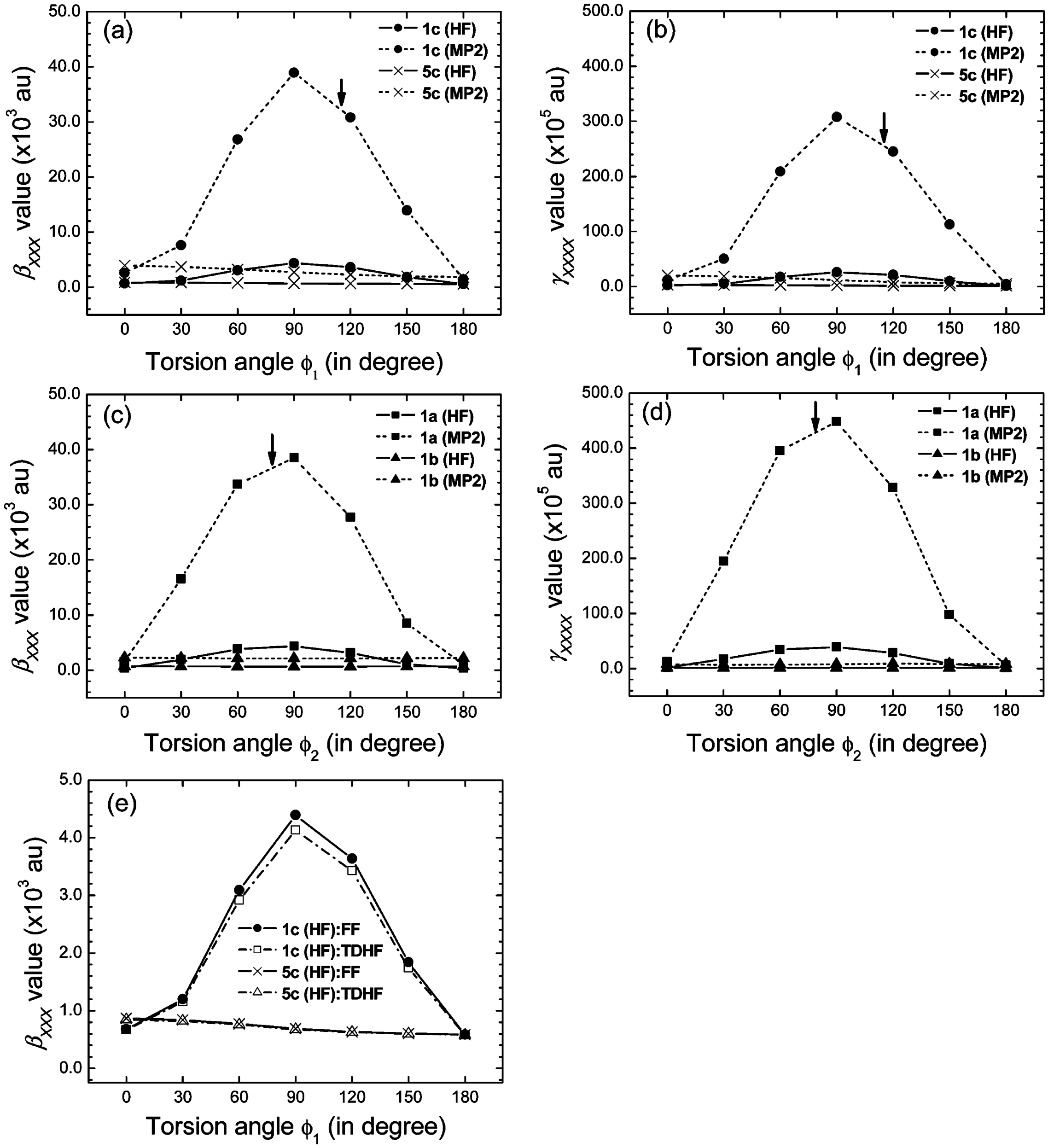

Figure 2. Torsion angle dependency on the hyperpolarizabilities in zwitterionic σ-systems by the FF method: (a) β_{XXX} for **1c** and **5c**, (b) γ_{XXXX} for **1c** and **5c**, (c) β_{XXX} for **1a** and **1b,** and (d) γ_{XXXX} for **1a** and **1b**. The FF calculations were performed at the levels of HF/6-31+G(d) and MP2/6-31+G(d) based on the HF/6-31G(d) optimized geometries. The arrows represent the optimized angle. Panel e shows the β_{XXX} comparison between the FF and TDHF methods in **1c** and **5c** at the HF/6-31+G(d)//HF/6-31G(d) level. All of the geometrical parameters except for the torsion angle were fixed in each panel.

the β_{XXX} values by the FF method well reproduced those by the TDHF method for both models. Therefore, it was confirmed that the β_{XXX} values of the zwitterionic σ-systems by the FF method were reasonable within the framework of the HF method.

Through-Space/-Bond Interaction Analysis of σ-Conjugation Effects on Hyperpolarizabilities. The TS/TB analysis was applied to model **1c** to examine the relationship between the σ-conjugations and hyperpolarizabilities in the zwitterionic σ-systems. The analysis was performed at the level of the 6-31+G(d) on the basis of the HF/6-31G(d) geometries. Table 7 shows the hyperpolarizabilities, β_{XXX}, γ_{XXXX}, and dipole moment μ_X of **1c** in "full interaction", "delete *d*-type", and "delete diffuse" states. The system has all the orbital interactions in the full interaction state, corresponding to the conventional calculation. The delete *d*-type and delete diffuse states were calculated by the TS/TB analysis to cut the σ-conjugations of the spacer unit in **1c**.

In the delete *d*-type state, we deleted the orbital interactions between the *d*-type functions at the C_3-C_4 position as shown in the structure at the bottom of Table 7. That is, the orbital interactions corresponding to all the combinations between *d*-functions belong to C_3 and those belonging to C_4 were eliminated by the TS/TB method, where the *d*-functions involve d_{XX}, d_{YY}, d_{ZZ}, d_{XY}, d_{XZ}, and d_{YZ} functions. In the delete *d*-type state, the β_{XXX} and γ_{XXXX} values decreased at both the HF and MP2 levels. However, the MP2/HF term for the β_{XXX} value did not change compared with that in the full interaction, and the MP2/HF term for the γ_{XXXX} value slightly increased. The absolute magnitude of the μ_X value was slightly reduced by the deletion. These results imply that the *d*-functions of the spacer unit make small contributions to the σ-conjugation, leading to

TABLE 7: Through-Space/-Bond Interaction Analysis of β_{XXX} (in $\times 10^3$ au), γ_{XXXX} (in $\times 10^5$ au), and Dipole Moment μ_X (in au) for 1c at the 6-31+G(d) Level[a]

	β_{XXX}			γ_{XXXX}			μ_X
state	HF	MP2[e]	MP2/HF[f]	HF	MP2[e]	MP2/HF[f]	HF
full interaction[b]	3.84	32.82	×8.5	22.23	259.97	×11.7	−14.59
Delete *d*-type[c]	2.69	22.96	×8.5	15.90	192.96	×12.1	−14.25
Delete diffuse[d]	−1.01	5.03	× (−5.0)	2.13	−6.58	× (−3.1)	−0.23

[a] All the analyses were performed on the basis of the HF/6-31G(d) optimized geometries. [b] System includes all the intramolecular interactions with no deletion. [c] The interactions between *d*-type functions at the C_3 and C_4 were deleted (see the structure below). [d] The interactions between diffuse functions at the C_3 and C_4 were deleted (see the structure below). [e] Frozen core approximation was adopted. [f] The ratio of the MP2 result to the HF result.

1c

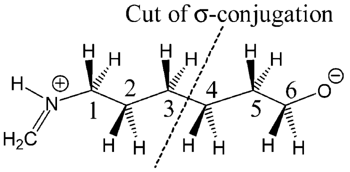

the small changes in both the charge distributions and hyperpolarizabilities.

In the delete diffuse state, the interactions between the diffuse functions at the C_3-C_4 position were deleted. In this case, we delete the orbital interactions corresponding to all the combinations between diffuse functions belong to C_3 and those belonging to C_4, where the diffuse functions involve the outermost *s*, p_X, p_Y, and p_Z functions in the 6-31+G(d) basis set. In the delete diffuse state, the β_{XXX}, γ_{XXXX}, and μ_X values remarkably decreased at both the HF and MP2 levels. It should be noted that an excess of the deletion for the σ-conjugation produced the negative but small absolute values of hyperpolarizabilities. The absolute magnitude of the MP2/HF terms for the β_{XXX} and γ_{XXXX} values also decreased compared with the full interaction and delete *d*-type results. This means that the deletions of the diffuse functions lead to nearly complete eliminations of the σ-conjugation effects due to large changes of the charge distributions. Therefore, it was concluded that the σ-conjugations based on the diffuse functions in the spacer unit produced the strong electron correlation effects on the hyperpolarizabilities observed in the 6-31+G(d) results.

The TS/TB analysis and the conformation analysis in the above subsection revealed that the unique behavior of the hyperpolarizabilities in the zwitterionic σ-systems results not from the summation of the local interactions in the acceptor and donor sides but from the $\pi-\sigma-\pi$ and (or) $\pi-\sigma-$n interactions through bond.

Conclusion

We theoretically examined the NLO properties of zwitterionic σ-systems concerning the electron correlation effects by using the ab initio MO calculations. Large electron correlation effects on the first- and second-order hyperpolarizabilities were found in the specific molecules with $\pi-\sigma-\pi$ and (or) $\pi-\sigma-$n type orbital interactions. It was found that the correlation effects strongly depend on the substituents, conformations, spacer size, and basis sets. Calculations with small basis sets and no correlation effects produce quantitatively incorrect values of the hyperpolarizabilities. In contrast, it was found that the HF results qualitatively predict the behavior of hyperpolarizabilities in the MP2 results. It is noteworthy that we can search NLO candidates showing the remarkable large hyperpolarizabilities at the MP2 level by small-cost HF level calculations. Moreover, the through-space/-bond interaction analysis was applied to the σ-conjugation effects in a zwitterionic σ-system. It was quantitatively revealed that the σ-conjugations on the spacer unit cause the large electron correlation effects on the hyperpolarizabilities.

Acknowledgment. This work was supported by the Precursory Research for Embryonic Science and Technology, Japan Science and Technology Agency (PRESTO, JST), and a grant-in-aid from the Ministry of Education, Culture, Sports, Science and Technology of Japan (MEXT). All the calculations were performed on the Linux PC clusters in our laboratory.

References and Notes

(1) Chopra, P.; Carlacci, L.; King, H. F.; Prasad, P. N. *J. Phys. Chem.* **1989**, *93*, 7120−7130.

(2) *Introduction to Nonlinear Optical Effects in Molecules and Polymers*; Prasad, P. N., Williams, D. J., Eds.; Wiley: New York, 1991.

(3) *Conjugated Polymers: The Novel Science and Technology of Highly Conducting and Nonlinear Optically Active Materials*; Brédas, J. L., Silbey, R. J., Eds.; Kluwer: Dordrecht, The Netherlands, 1991.

(4) Shelton, D. P.; Rice, J. E. *Chem. Rev.* **1994**, *94*, 3−29.

(5) Burland, D. M.; Miller, R. D.; Walsh, C. A. *Chem. Rev.* **1994**, *94*, 31−75.

(6) Kanis, D. R.; Ratner, M. A.; Marks, T. J. *Chem. Rev.* **1994**, *94*, 195−242.

(7) Brédas, J. L.; Adant, C.; Tackx, P.; Persoons, A.; Pierce, B. M. *Chem. Rev.* **1994**, *94*, 243−278.

(8) *Nonlinear Optical Materials: Theory and Modelling*; Karna, S. P., Yeates, A. T., Eds.; ACS Symposium Series, Vol. 628; American Chemical Society: Washington, D.C., 1996.

(9) Nakano, M.; Yamada, S.; Shigemoto, I.; Yamaguchi, K. *Chem. Phys. Lett.* **1996**, *251*, 381−386.

(10) van Hutten, P. F.; Hadziioannou, G.; Bursi, R.; Feil, D. *J. Phys. Chem.* **1996**, *100*, 85−94.

(11) Abe, J.; Shirai, Y.; Nemoto, N.; Miyata, F.; Nagase, Y. *J. Phys. Chem. B* **1997**, *101*, 576−582.

(12) Gu, F. L.; Aoki, Y.; Imamura, A.; Bishop, D. M.; Kirtman, B. *Mol. Phys.* **2003**, *101*, 1487−1494.

(13) Jacquemin, D.; André, J.-M.; Perpète, E. A. *J. Chem. Phys.* **2004**, *121*, 4389−4396.

(14) Song, N.; Men, L.; Gao, J. P.; Bai, Y.; Beaudin, A. M. R.; Yu, G.; Wang, Z. Y. *Chem. Mater.* **2004**, *16*, 3708−3713.

(15) Liao, Y.; Bhattacharjee, S.; Firestone, K. A.; Eichinger, B. E.; Paranji, R.; Anderson, C. A.; Robinson, B. H.; Reid, P. J.; Dalton, L. R. *J. Am. Chem. Soc.* **2006**, *128*, 6847−6853.

(16) Xu, H.-L.; Li, Z.-R.; Wu, D.; Wang, B.-Q.; Li, Y.; Gu, F. L.; Aoki, Y. *J. Am. Chem. Soc.* **2007**, *129*, 2967−2970.

(17) Tsai, H.-C.; Yu, I.-C.; Chang, P.-H.; Yu, D.-C.; Hsiue, G.-H. *Macromol. Rapid Commun.* **2007**, *28*, 334−339.

(18) Yesudas, K.; Bhanuprakash, K. *J. Phys. Chem. A* **2007**, *111*, 1943−1952.

(19) Albert, I. D. L.; Marks, T. J.; Ratner, M. A. *J. Phys. Chem.* **1996**, *100*, 9714−9725.

(20) Morley, J. O. *THEOCHEM* **1996**, *365*, 1−7.

(21) Smith, G. J.; Dunford, C. L.; Kay, A. J.; Woolhouse, A. D. *J. Photochem. Photobiol., A* **2006**, *179*, 237−242.

(22) Kogej, T.; Meyers, F.; Marder, S. R.; Silbey, R.; Brédas, J. L. *Synth. Met.* **1997**, *85*, 1141−1142.

(23) Verbiest, T.; Houbrechts, S.; Kauranen, M.; Clays, K.; Persoons, A. *J. Mater. Chem.* **1997**, *7*, 2175−2189.

(24) Albert, I. D. L.; Marks, T. J.; Ratner, M. A. *J. Am. Chem. Soc.* **1997**, *119*, 6575−6582.

(25) Jacquemin, D.; Champagne, B.; André, J.-M. *Int. J. Quantum Chem.* **1997**, *65*, 679−688.

(26) Kirtman, B.; Champagne, B.; Gu, F. L.; Bishop, D. M. *Int. J. Quantum Chem.* **2002**, *90*, 709−718.

(27) Geskin, V. M.; Lambert, C.; Brédas, J.-L. *J. Am. Chem. Soc.* **2003**, *125*, 15651−15658.

(28) Geskin, V. M.; Bredas, J. L. *Int. J. Quantum Chem.* **2003**, *91*, 303−310.

(29) Ohnishi, S.; Gu, F. L.; Naka, K.; Imamura, A.; Kirtman, B.; Aoki, Y. *J. Phys. Chem. A* **2004**, *108*, 8478−8484.

(30) Champagne, B.; Botek, E.; Nakano, M.; Nitta, T.; Yamaguchi, K. *J. Chem. Phys.* **2005**, *122*, 114315.

(31) Sainudeen, Z.; Ray, P. C. *J. Phys. Chem. A* **2005**, *109*, 9095−9103.

(32) Torres, E. M.; Fonseca, T. L.; Esteves, C. S.; Amaral, O. A. V.; Castro, M. A. *Chem. Phys. Lett.* **2005**, *403*, 268−274.

(33) Fonseca, T. L.; de Oliveira, H. C. B.; Amaral, O. A. V.; Castro, M. A. *Chem. Phys. Lett.* **2005**, *413*, 356−361.

(34) Andreu, R.; Blesa, M. J.; Carrasquer, L.; Garín, J.; Orduna, J.; Villacampa, B.; Alcalá, R.; Casado, J.; Delgado, M. C. R.; Navarrete, J. T. L.; Allain, M. *J. Am. Chem. Soc.* **2005**, *127*, 8835−8845.

(35) Beaudin, A. M. R.; Song, N.; Bai, Y.; Men, L.; Gao, J. P.; Wang, Z. Y.; Szablewski, M.; Cross, G.; Wenseleers, W.; Campo, J.; Goovaerts, E. *Chem. Mater.* **2006**, *18*, 1079−1084.

(36) Schuddeboom, W.; Krijnen, B.; Verhoeven, J. W.; Staring, E. G. J.; Rikken, G. L. J. A.; Oevering, H. *Chem. Phys. Lett.* **1991**, *179*, 73−78.

(37) Albert, I. D. L.; Marks, T. J.; Ratner, M. A. *J. Am. Chem. Soc.* **1997**, *119*, 3155−3156.

(38) Albert, I. D. L.; Marks, T. J.; Ratner, M. A. *J. Am. Chem. Soc.* **1998**, *120*, 11174−11181.

(39) Fort, A.; Boeglin, A.; Mager, L.; Amyot, C.; Combellas, C.; Thiébault, A.; Rodriguez, V. *Synth. Met.* **2001**, *124*, 209−211.

(40) Keinan, S.; Zojer, E.; Brédas, J.-L.; Ratner, M. A.; Marks, T. J. *THEOCHEM* **2003**, *633*, 227−235.

(41) Isborn, C. M.; Davidson, E. R.; Robinson, B. H. *J. Phys. Chem. A* **2006**, *110*, 7189−7196.

(42) Kang, H.; Facchetti, A.; Jiang, H.; Cariati, E.; Righetto, S.; Ugo, R.; Zuccaccia, C.; Macchioni, A.; Stern, C. L.; Liu, Z.; Ho, S.-T.; Brown, E. C.; Ratner, M. A.; Marks, T. J. *J. Am. Chem. Soc.* **2007**, *129*, 3267−3286.

(43) Bhanuprakash, K.; Rao, J. L. *Chem. Phys. Lett.* **1999**, *314*, 282−290.

(44) Rao, J. L.; Bhanuprakash, K. *THEOCHEM* **1999**, *458*, 269−273.

(45) Sitha, S.; Rao, J. L.; Bhanuprakash, K.; Choudary, B. M. *J. Phys. Chem. A* **2001**, *105*, 8727−8733.

(46) Orimoto, Y.; Aoki, Y. *Phys. Rev. A* **2003**, *68*, 063808.

(47) Imamura, A.; Sugiyama, H.; Orimoto, Y.; Aoki, Y. *Int. J. Quantum Chem.* **1999**, *74*, 761−768.

(48) Orimoto, Y.; Aoki, Y. *Int. J. Quantum Chem.* **2002**, *86*, 456−467.

(49) Orimoto, Y.; Aoki, Y. *Int. J. Quantum Chem.* **2003**, *92*, 355−366.

(50) Orimoto, Y.; Naka, K.; Takeda, K.; Aoki, Y. *Org. Biomol. Chem.* **2005**, *3*, 2244−2249.

(51) Orimoto, Y.; Naka, K.; Aoki, Y. *Int. J. Quantum Chem.* **2005**, *104*, 911−918.

(52) Orimoto, Y.; Aoki, Y. *J. Polym. Sci., Part B: Polym. Phys.* **2006**, *44*, 119−133.

(53) Orimoto, Y.; Imai, T.; Naka, K.; Aoki, Y. *J. Phys. Chem. A* **2006**, *110*, 5803−5808.

(54) Kurtz, H. A.; Stewart, J. J. P.; Dieter, K. M. *J. Comput. Chem.* **1990**, *11*, 82−87.

(55) GAMESS: Schmidt, M. W.; Baldridge, K. K.; Boatz, J. A.; Elbert, S. T.; Gordon, M. S.; Jensen, J. H.; Koseki, S.; Matsunaga, N.; Nguyen, K. A.; Su, S. J.; Windus, T. L.; Dupuis, M.; Montgomery, J. A. *J. Comput. Chem.* **1993**, *14*, 1347−1363.

(56) Karna, S. P.; Dupuis, M. *J. Comput. Chem.* **1991**, *12*, 487−504.

(57) Pople, J. A.; Binkley, J. S.; Seeger, R. *Int. J. Quantum Chem.* **1976**, *S10*, 1−19.

(58) Frisch, M. J.; Trucks, G. W.; Schlegel, H. B.; Scuseria, G. E.; Robb, M. A.; Cheeseman, J. R.; Montgomery, J. A., Jr.; Vreven, T.; Kudin, K. N.; Burant, J. C.; Millam, J. M.; Iyengar, S. S.; Tomasi, J.; Barone, V.; Mennucci, B.; Cossi, M.; Scalmani, G.; Rega, N.; Petersson, G. A.; Nakatsuji, H.; Hada, M.; Ehara, M.; Toyota, K.; Fukuda, R.; Hasegawa, J.; Ishida, M.; Nakajima, T.; Honda, Y.; Kitao, O.; Nakai, H.; Klene, M.; Li, X.; Knox, J. E.; Hratchian, H. P.; Cross, J. B.; Adamo, C.; Jaramillo, J.; Gomperts, R.; Stratmann, R. E.; Yazyev, O.; Austin, A. J.; Cammi, R.; Pomelli, C.; Ochterski, J. W.; Ayala, P. Y.; Morokuma, K.; Voth, G. A.; Salvador, P.; Dannenberg, J. J.; Zakrzewski, V. G.; Dapprich, S.; Daniels, A. D.; Strain, M. C.; Farkas, O.; Malick, D. K.; Rabuck, A. D.; Raghavachari, K.; Foresman, J. B.; Ortiz, J. V.; Cui, Q.; Baboul, A. G.; Clifford, S.; Cioslowski, J.; Stefanov, B. B.; Liu, G.; Liashenko, A.; Piskorz, P.; Komaromi, I.; Martin, R. L.; Fox, D. J.; Keith, T.; Al-Laham, M. A.; Peng, C. Y.; Nanayakkara, A.; Challacombe, M.; Gill, P. M. W.; Johnson, B.; Chen, W.; Wong, M. W.; Gonzalez, C.; Pople, J. A. *Gaussian 03*, Revision C.02; Gaussian, Inc.: Wallingford, CT, 2004.